Available online at www.sciencedirect.com
SCIENCE DIRECT®
International Journal of Fatigue 25 (2003) 585–595
International Journal of Fatigue
www.elsevier.com/locate/ijfatigue

Numerical procedure for predicting the rolling contact fatigue crack initiation

M. Šraml *, J. Flašker, I. Potrč

University of Maribor, Faculty of Mechanical Engineering, Smetanova 17, 2000 Maribor, Slovenia

Received 18 July 2002; received in revised form 5 December 2002; accepted 19 December 2002

Abstract

A computational numerical model for contact fatigue damage analysis of mechanical elements is presented in this paper. The computational approach is based on continuum mechanics, where a homogenous and elastic material model is assumed in the framework of the finite element method analysis. Cyclic contact loading conditions are simulated with moving Hertzian contact pressure. The time-depending loading cycles are defined for each observed material point on and under the contact area. Furthermore, the influence of friction upon rolling–sliding contact loading cycles is analysed in detail, using Coulomb's friction law. The model for prediction of the number of loading cycles, required for initial fatigue damages to appear, is based on Coffin–Manson relations between deformations and loading cycles, and includes characteristic material fatigue parameters. As a general example, the model is used to analyse a fundamental contact problem of a cylinder and flat surface, which is usually a substitutional model for analysing real mechanical problems. However, the results concerning the identification of critical material points and the number of loading cycles, required for initial fatigue damages to appear at those points, are the main purpose of the presented study.
© 2003 Elsevier Science Ltd. All rights reserved.

Keywords: Contact fatigue; Crack initiation; Numerical modelling

1. Introduction

Mechanical behaviour of various machine elements, such as gears, brakes, clutches, rolling bearings, wheels, rails, screw and riveted joints, couplings—are influenced by interaction between contact elements and surfaces. Surfaces in rolling and/or sliding contact are exposed to material contact fatigue. Contact fatigue can be defined as a kind of damage caused by changes in the material microstructure which result, initially, in crack initiation and then in crack propagation, under the influence of time-dependent rolling and/or sliding contact loads. Contact fatigue process can be in general divided into two main parts: (i) initiation of micro-cracks due to local accumulation of dislocations, high stresses at local points, plastic deformation around inhomogeneous inclusions or other imperfections in or under the contact surface; (ii) crack propagation, which causes permanent damage to a mechanical element, i.e. the exceeding of fracture toughness of the material [5,18,21].

Contact fatigue is extremely important for engineering applications involving localized contacts (see Ekberg [3,4], Flašker et al. [6], Glodež et al. [7]). The repeated rolling and/or sliding contact conditions cause permanent damage to the material due to accumulation of deformation. An overview of existing models for fatigue damage and life prediction for homogeneous materials is shown in Fatemi [5]. It should be mentioned, although modelling of contact fatigue initiation is often supported by experimental investigations, that most of the work published on contact fatigue is theoretical [1,2,5,12]. Works by Mura and Nakasone [12] and by Cheng et al. [2] represent a large step forward in the field of developing physical and mathematical models concerning fatigue damage initiation. Practical applicability of those models in engineering practice is, however, limited to a certain extent. A large number of different material and geometric parameters is needed to be determined for calculation of the number of loading cycles for fatigue

* Corresponding author. Tel.: +386-2-220-7722; fax: +386-2-220-7729.
E-mail address: sraml.matjaz@uni-mb.si (M. Šraml).

0142-1123/03/$ - see front matter © 2003 Elsevier Science Ltd. All rights reserved.
doi:10.1016/S0142-1123(03)00019-7

Nomenclature

a	Half- width of Hertzian contact
b	Exponent of material strength
c	Fatigue ductility exponent
p_0	Maximum Hertzian pressure
$p(x)$	Normal Hertzian pressure
$q(x)$	Tangential Hertzian pressure
n'	Material hardening exponent
t	Time
D	Ductility factor
$E_{1,2}$	Young's modulus
$E*$	Equivalent Young's modulus
F_N	Normal contact force per unit length
K'	Material strength coefficient
N_f	Number of loading cycles for crack initiation
$R*$	Equivalent radius of contacting cylinders
x_i, y_i	Location of observed material point, coordinates
μ	Coefficient of friction
$\nu_{1,2}$	Poisson's ratio
ε'_f	Fatigue ductility coefficient
ε_a	Strain amplitude
$\Delta\varepsilon$	Deformation range
$\Delta\varepsilon_1$	Amplitude of maximum principal deformation
$\Delta\varepsilon_p$	Plastic deformation range
σ_m	Mean value of stress
σ_{UTS}	Ultimate tensile stress
σ_Y	Yield stress
$\Delta\sigma$	Stress range
σ_a	Alternating stress amplitude
σ_h	Hydrostatic stress
σ'_f	Fatigue strength coefficient
σ_1	Principal stress
σ_1^{max}	Max. value of principal stresses
τ_{xy}	Shear stress
BEM	Boundary element method
FEM	Finite element method
HCF	High cycle fatigue
LCF	Low cycle fatigue
PSB	Persistent slip bands
SWT	Smith-Watson-Topper method
T	Transition point

damage initiation [2]. Additionally, those parameters differ for different materials, geometries and loading spectra [2,9]. The applicability of analytical methods is limited to idealised engineering problems and they are based upon well known theoretical methods for determining fatigue damage initiation strain–life methods: Coffin–Manson's hypothesis, Morrow's analysis, Smith–Watson–Topper (SWT) method, etc. [1,5,18,21]. Computational approaches to fatigue initiation analyses are based upon the method which determines the ratio between the specific deformation and the number of loading cycles, often referred to as local stress–strain method [5,18,21]. Lately, a connection between the results, obtained by means of the finite element method (FEM) and/or the boundary element method (BEM), and those, obtained by the analyses of material fatigue can be traced [13,16,19,20]. The connection between numerical results and those obtained by experimentally determined fatigue parameters represents the basis for determining the changes in the micro-level of the material structure which causes material hardening or softening and the phenomenon of residual stresses (tensile, compressive)

[6,13,17,21]. The significance of dealing with different mechanical elements and constructions and different approaches to sizing and endurance control prove that those problems are of great interest today [3,6,15].

Modelling of contact fatigue crack initiation is the main concern of this paper. So far there is no adequate computational model available that would enable description of the fatigue crack initiation, based on the stress analysis of the contact problem with the use of appropriate material fatigue parameters. The purpose of the present study is to present a model for prediction of contact fatigue initiation, which is based on continuum mechanics, cyclic contact loading and characteristic material fatigue parameters. The material model is assumed as homogeneous, without imperfections such as inclusions, asperities, roughness, residual stresses etc. as often occur in mechanical elements. Moving contact load is often used for simulation of the cyclic loading in fatigue crack initiation analyses on mechanical elements. Also, the influence of friction between the contact surfaces and fatigue initiation is examined in detail.

2. Description of the contact fatigue crack initiation model

A comprehensive model for contact fatigue life prediction of mechanical elements should consider the time history of applied contact loads, regarding their range of variation. The rolling–sliding contact loads, typical for mechanical elements such as gears, wheels and rails, rolling bearings etc., are generally stochastic in a certain range, due to the stochastic character of some contact parameters. For a description of a general case of contact loading, one has to estimate average normal and tangential contact forces for computational determination of surface and subsurface contact stresses. Normal contact forces can be appropriately determined by the Hertzian contact theory [8], while the tangential frictional forces can be considered with the Coulomb friction law. By applying these contact loading conditions in a moving fashion along the contact area of the computational model, one can computationally determine the stress loading cycle for each observed material point (x_i, y_i) on or under the contact surface (Fig. 1). That way, a realistic description of a stress cyclic loading in the time domain due to rolling and/or sliding contact conditions is achieved. A finite or boundary element method can be used for this purpose [14], [20]. In this study, the FE analysis program MSC/Nastran has been used for computational estimation of the loading cycles [11].

The complete procedure for computational determination of the material point stress loading cycle can be described as follows.

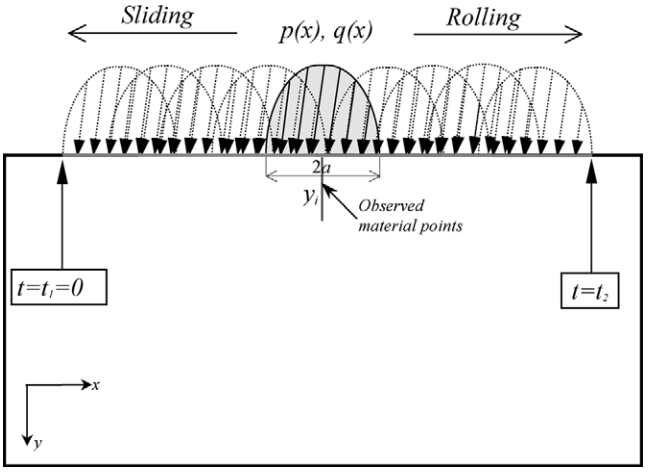

Fig. 1. General idea for determination of the loading cycle at contact fatigue of mechanical elements.

2.1. Generation of the generalised contact model

The actual contact problem is transformed into its generalised form with use of Hertzian theory (see Johnson [8]), i.e. the equivalent contact cylinder is generated from the curvature radii of the considered contacting mechanical elements at the point of actual contact. The equivalent Young's modulus and Poisson's ratio are also computed from respective data of contacting bodies [8]; see Fig. 2.

According to the Hertzian theory, the distribution of normal contact pressure in the contact area can be determined by [8]

$$p(x) = \frac{2F_N}{\pi a}\sqrt{1-\frac{x^2}{a^2}}, \tag{1}$$

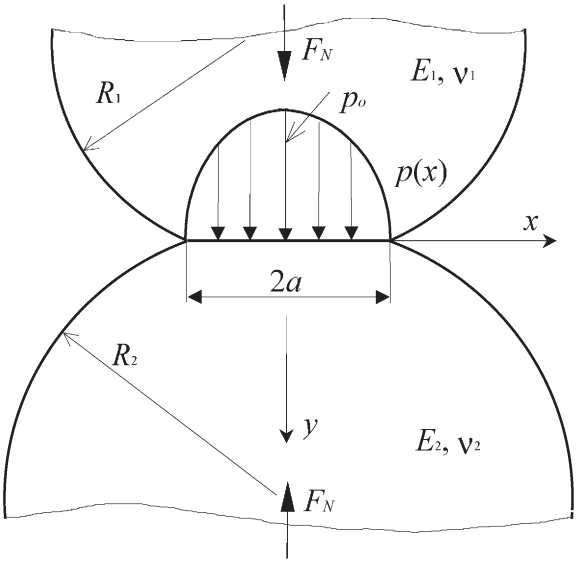

Fig. 2. Equivalent model of two contacting cylinders [8].

where F_N is the normal contact force per unit width, a is half length of the contact area, which can be determined from [8]

$$a = \sqrt{\frac{4F_N R^*}{\pi E^*}}, \tag{2}$$

where $E*$ and $R*$ are the equivalent Young's elastic modulus and the equivalent radius, respectively, defined as [8]

$$\frac{1}{E^*} = \frac{1-\nu_1^2}{E_1} + \frac{1-\nu_2^2}{E_2}, \tag{3}$$

$$\frac{1}{R^*} = \frac{1}{R_1} + \frac{1}{R_2}, \tag{4}$$

where E_1, R_1, ν_1 and E_2, R_2, ν_2 are the Young's modulus, the curvature radii and Poisson's ratio of contacting cylinders, see Fig. 2. The maximum contact pressure $p_0=p(x=0)$ can than be determined as [8]

$$p_0 = \sqrt{\frac{F_N E^*}{\pi R^*}}. \tag{5}$$

In the analysing of real mechanical components, some partial sliding occurs during time-dependent contact loading, which can originate from different effects (complex loading conditions, geometry, surface, etc.) and it is often modelled with traction force due to the pure Coulomb friction law [8]. In the analysed case frictional contact loading $q(x)$ is a result of the tractive force action (tangential loads) due to the relative sliding of the contact bodies and is here determined by utilising the previously mentioned Coulomb friction law [8]

$$q(x) = \mu \cdot p(x), \tag{6}$$

where μ is the coefficient of friction between contacting bodies.

For the general case of elastic contact between two deformable bodies in a standing situation, the analytical solutions are well known. However, using general Hertzian equations [8] it is hard to provide the loading cycle history and/or simulation of a contact pressure distribution of moving contact in the analytical manner. Therefore, the finite element method is used for simulating two-dimensional friction contact loading in this case and the same procedure is usually used when dealing with complex contact loading conditions (e.g. in the case of gears analysis).

The equivalent contact model is spatially discretised in the region of interest, where finer mesh is used around material points (x_i, y_i) on and under the contact region. The computational model for evaluating contact stresses is a two-dimensional rectangle, with assumed plain strain conditions (Fig. 3).

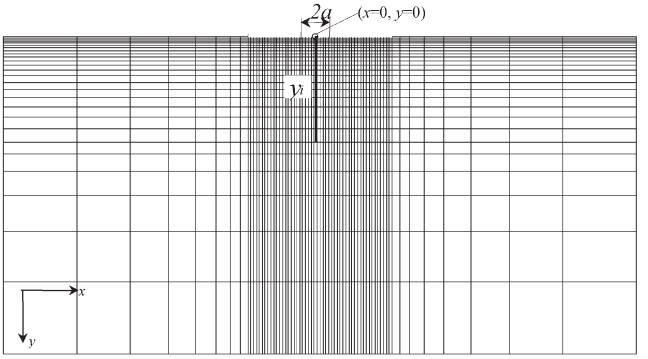

Fig. 3. Finite element model for determination of contact loading cycles.

2.2. Generation of contact loading conditions

The loading boundary conditions comprise the Hertzian normal contact loading distribution and tangential contact loading due to frictional forcers in the contact. The loading is moving along the contact surface of the generalised computational model.

2.3. Computational determination of a stress loading cycle during moving contact load

The stress analysis of the generalised contact model is performed in the framework of the finite element method. The appropriate stress state for each observed material point is computed for each position of the moving contact loading. This procedure results in generation of real stress loading cycles of material points in one pass of the rolling–sliding contact, which are necessary for the following contact fatigue analysis.

2.4. Determination of conditions for fatigue crack initiation analysis

When the stress loading cycles are determined, the fatigue analysis for each observed material point could be performed. The methods for fatigue analysis are most frequently based on the relation between deformations, stresses and number of loading cycles and are usually modified to fit the nature of the stress cycle, e.g. repeated or reversed stress cycle (see Suresh [18], Zahavi and Torbilo [21]). The number of stress cycles required for a fatigue crack to appear can be determined iteratively with the strain–life method $\varepsilon-N$, where the relationship between the specific deformation increment $\Delta\varepsilon$ and the number of loading cycles N_f is fully characterized with the following equation [18,21]

$$\frac{\Delta\varepsilon}{2} = \frac{\sigma_a}{E} + \frac{\Delta\varepsilon_p}{2} = \frac{\sigma'_f}{E}(2N_f)^b + \varepsilon'_f(2N_f)^c, \tag{7}$$

where σ'_f is the fatigue strength coefficient, b the

strength exponent, ε'_f the fatigue ductility coefficient and c the fatigue ductility exponent. Generally, the following modified approaches of the strain–life method are most often in use for fatigue calculations: Coffin–Manson's hypothesis ($\varepsilon-N$ method), Morrow's analysis, Smith–Watson–Topper (SWT) method (see [18,21]). According to Morrow, the relationship between strain amplitude, ε_a, and the pertinent number of load cycles to failure, N_f, can be written as [18,21]

$$\varepsilon_a = \frac{\sigma'_f}{E}(2N_f)^b + \varepsilon'_f(2N_f)^c, \tag{8}$$

where E is the elastic modulus, σ'_f is the fatigue strength coefficient, ε'_f is the fatigue ductility coefficient, b is the exponent of strength and c is the fatigue ductility exponent, respectively.

Morrow equation with mean stress, σ_m, correction (with a static mean stress not equal 0) [21]

$$\varepsilon_a = \frac{(\sigma'_f-\sigma_m)}{E}(2N_f)^b + \varepsilon'_f(2N_f)^c, \tag{9}$$

According to Coffin–Manson, this relationship can be simplified as

$$\varepsilon_a = 1{,}75\frac{\sigma_{UTS}}{E}N_f^{-0.12} + 0.5D^{0.6}N_f^{-0.6}, \tag{10}$$

where σ_{UTS} is ultimate tensile stress and D is the ductility, defined as

$$D = \ln\frac{A_0}{A_{fracture}} \cong \varepsilon_{fracture}.$$

The Smith–Watson–Topper method considers the influence of mean stress value and can be defined as [21]

$$\sigma_1^{max}\frac{\Delta\varepsilon_1}{2} = \sigma'_f\varepsilon'_f(2N_f)^{b+c} + \frac{\sigma'^2_f}{E}(2N_f)^{2b}, \tag{11}$$

where $\Delta\varepsilon_1$ is the amplitude of maximum principal deformation and σ_1^{max} is the maximum value of principal stresses in the direction of maximum principal deformation.

All the described fatigue life models, used in this work, are actually based on the strain life method. Once a local stress or strain–time history has been established a fatigue analysis method must be applied. Furthermore, material properties are introduced as "material fatigue data" from tests (see Table 2) [10]. The strain–life approach can be used as advantage over the S–N method even in high cycle application, due to its less scatter-prone materials data. Assumptions that have been made at fatigue life models are the following: the models are uni-axial, which means that just one principal stress occurs in one direction (single stress vector).

Before damage can be determined and summed for each cycle certain corrections need to take place, the main correction being the conversion of purely elastic stresses and strains to elasto–plastic stresses and strains. In this work, plasticity is accounted for in the crack initiation method by the Neuber method [13, 18]. The elastic stresses and strains are looked up on the elastic line and then corrected to fall onto the cyclic stress–strain curve to determine the elastic–plastic stresses and strains. It is then this elastic–plastic strain that is used to look up damage on the strain–life damage curve. Neuber's elastic–plastic correction is based on the simple principle that the product of the elastic stress and strain should be equal to the product of the elastic–plastic stress and strain from the cyclic stress–strain curve (Eq. (12)) [18].

$$\frac{\Delta\varepsilon}{2} = \frac{\sigma}{2E} + \left[\frac{\Delta\sigma}{2K'}\right]^{1/n'} \tag{12}$$
$$\Delta\sigma\cdot\Delta\varepsilon = E\Delta\varepsilon_e^2$$

where $\Delta\varepsilon$, $\Delta\sigma$ are incremental values of strain and stress, E is the elastic modulus, $\Delta\varepsilon_e$ is incremental value of elastic strain, n' is the material hardening exponent and K' is the material strength coefficient. Through an iterative method, the elastic–plastic stress and strain can be determined.

The material curve (Fig. 4) can be fully characterized by knowing previously described material parameters σ'_f, b, ε'_f, c as shown in eq. (7) and depends on which method of analysis is used. This curve is devided into an elastic component and a plastic component, which can also be plotted separately.

The transition point T (Fig. 4) defines the difference between high cycles fatigue (HCF) versus low cycles fatigue (LCF) regime. Generally, there is no irreversible deformation in the high-cycle fatigue regime (HCF) at the macroscopic level, while the low-cycle fatigue regime (LCF) implies significant macroscopic deformation conducting to irreversible deformation already at this level [18]. Anyway, the first microcracks in the persistent slip bands (PSB) appear quite early in the life

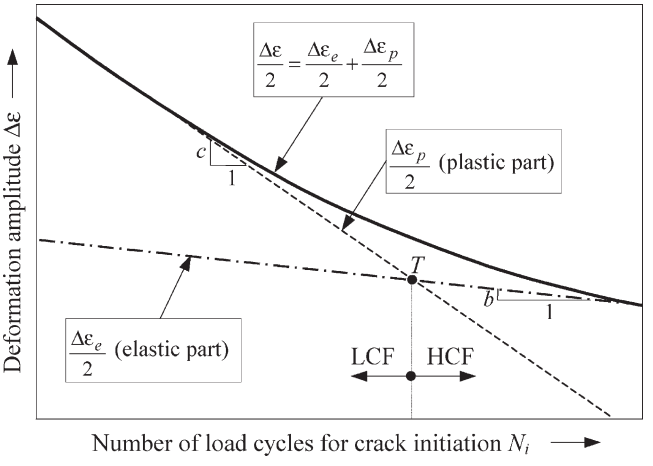

Fig. 4. Strain–life method for the fatigue crack initiation.

of the mechanical component, regardless of the fatigue regime [18]. The strain and the plastic strain are no more related to the stress through a simple relation. However, the strain–life method $\varepsilon-N$ is not an ideal model for fatigue damage initiation analysis at the microstructural level, since the micro-crack initiation in crystal grains and dislocation theory are not taken into account. It has been established in the work of Suresh [18] and Bhattacharya et al. [1] that fatigue damage initiation is represented by the transition of a certain number of loading cycles when the first fatigue damage occurs, on the basis of the assumed initial homogenous state of the material. Thus, the $\varepsilon-N$ method represents a very useful method for determination of the initial fatigue damage, which is located at the material point with the largest stresses, where fatigue damage initiation is most probable to occur in the time domain.

3. Practical application

The fundamental contact problem of a cylinder and flat surface was used as a practical example [8]. An elastic and isotropic material model, without material imperfections or initial damage was assumed, with the geometric, material and boundary conditions data used shown in Table 1. These parameters were used because in the substitutional Hertzian models of existing gear pairs the same data appear [6,15]. The finite element model, used for determination of the contact stresses and determination of stress loading cycles, is shown in Fig. 3. By applying the procedure for computational determination of the material point stress loading cycle, as described in Section 2, it is possible to examine the influence of friction on the stress loading cycle and the material fatigue process [20].

The results of the generalised contact model are the course of the standardized loading cycles in respect to various stress components (σ_x, σ_y, τ_{xy}), representative stress states like Tresca, the largest principal stresses (σ_1) and hydrostatic stresses (σ_h) [19,20]. The Tresca loading cycle is most often used for fatigue analyses and is based on the equivalent shear stresses, which is a function of deviatoric stresses and equals the largest of the principal shear stresses. Considering the fact that contact fatigue is, to a large extent, influenced by contact surface roughness and friction (regardless of its origin), the influence of friction on the course of a loading cycle has been analysed. The influence of the friction coefficient on the course of contact stresses on and under the contact surface (at static contact) is shown in Fig. 5. Generally, when dealing with comparative Tresca stresses, the influence of the friction coefficient is essential: in the case of no friction (μ=0) the maximum value of normalised contact stresses is placed under the contact (x_i=0 mm, y_i=−0,20784 mm) and the "maximum value point" then moves towards the contact surface due to increased friction. Extreme values of friction coefficients (μ=0.3–0.5) are analysed due to investigation of the general influence of friction on the contact fatigue process.

The results of the determined contact loading cycles, with emphasis on the influence of friction, are shown next. The comparative Tresca based loading cycles are first presented. The influence of friction (traction contact force) on the course of the loading cycles at the contact surface is of essential meaning (Fig. 6(a)).

Figs 6(a), (b) and (c) show clear dependence of the computed Tresca stress cycles on various coefficients of friction at different material points, one on the contact surface (Fig. 6(a)) and the other at some depth under the contact surface (Fig. 6(b) and (c)). The influence of friction is most outstanding on the contact surface (x_i, y_i=0 mm), where higher friction results in higher relative contact loading (Tresca stresses normalised with p_0), and is receding with the depth under the contact surface. Computational analyses have shown that the influence of friction can be neglected at depths larger than $1.4 \cdot a$ (Fig. 5). This limit corresponds to the position of the material

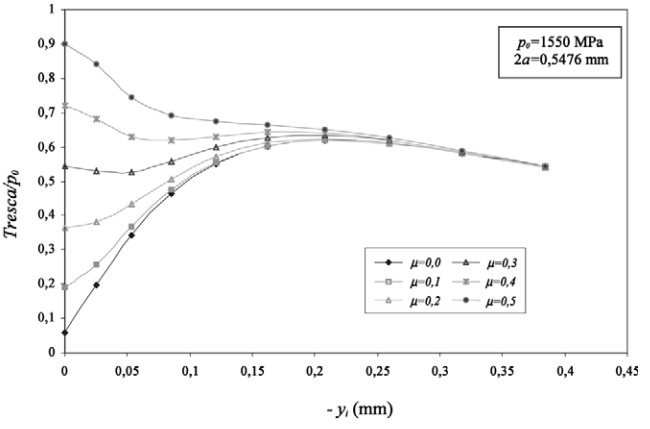

Fig. 5. Tresca comparative stresses under the contact surface (x=0 mm, y_i).

Table 1
Material and geometric parameters of the generalised contact model

Maximum contact pressure p_0 (MPa)	Young's modulus E_1=E_2 (GPa)	Poisson's ratio ν_1=ν_2	Contact width 2a (mm)	Coefficient of friction μ
1550	2.07	0.3	0.5476	(0.0–0.5)$\Delta\mu$=0.1

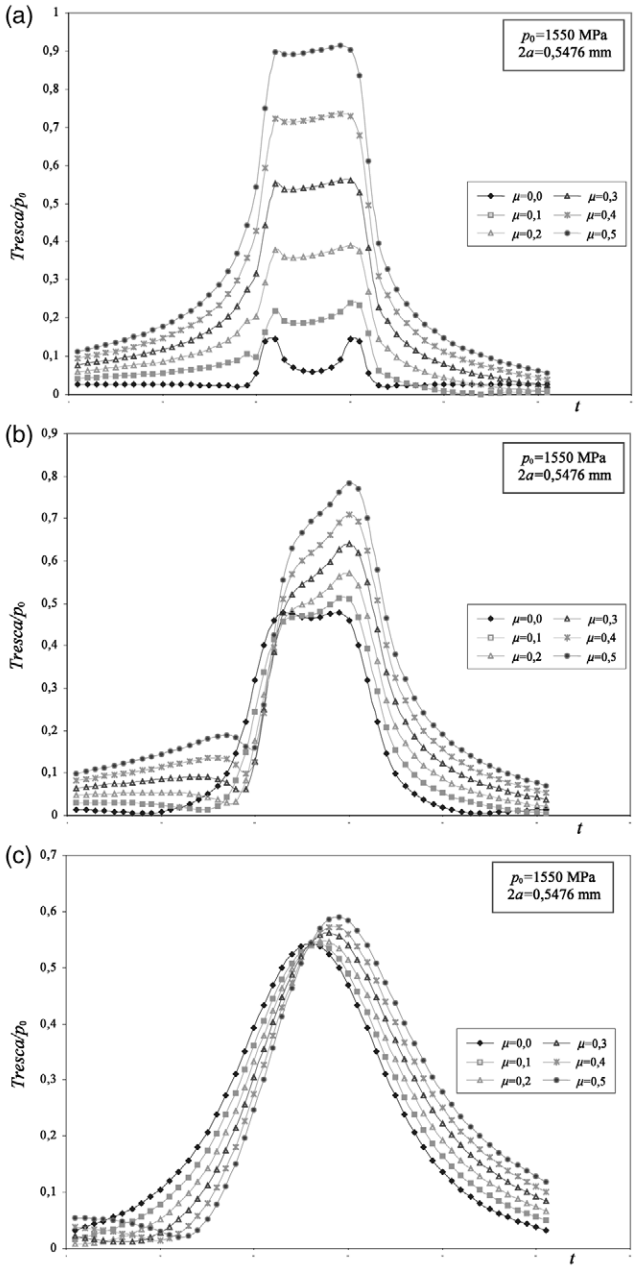

Fig. 6. (a) Tresca comparative stress cycles, on the contact surface (x_i, y_i=0 mm); (b) Tresca comparative stress cycles, under the contact surface (x_i, y_i=−0.08523 mm) (c) Tresca comparative stress cycles, under the contact surface (x_i, y_i=−0.38420 mm).

point (x_i, y_i=−0.3842 mm) for the presented example (see Fig. 5).

The shear stress based loading cycles are presented next. At contact loading, shear stresses could play an essential role for the stress–strain field at the homogeneous model of fatigue crack initiation life prediction [7,8,18]. The influence of friction on the position of maximum relative stresses (compressive and tensile) is the following: the maximum values appear on the contact surface (x_i, y_i=0 mm) for the traction coefficient ranging from 0.3 to 0.5, with the extreme values of (τ_{xy}/p_0=0.3–0.45) corresponding to the largest values of the traction coefficient (see Fig. 7(a)). The influence of the friction coefficient is reduced under the contact surface and also the relative values of loads are lower at these points (Figs 7(b) and (c)). Anyway, the analogous conclusion can be observed when comparing comparative based time-dependent loading cycles (Figs 6(a), (b) and (c)) and statically calculated contact stresses (comparative Tresca stresses, Fig. 5), the maximum relative values at the lowest friction coefficients are placed

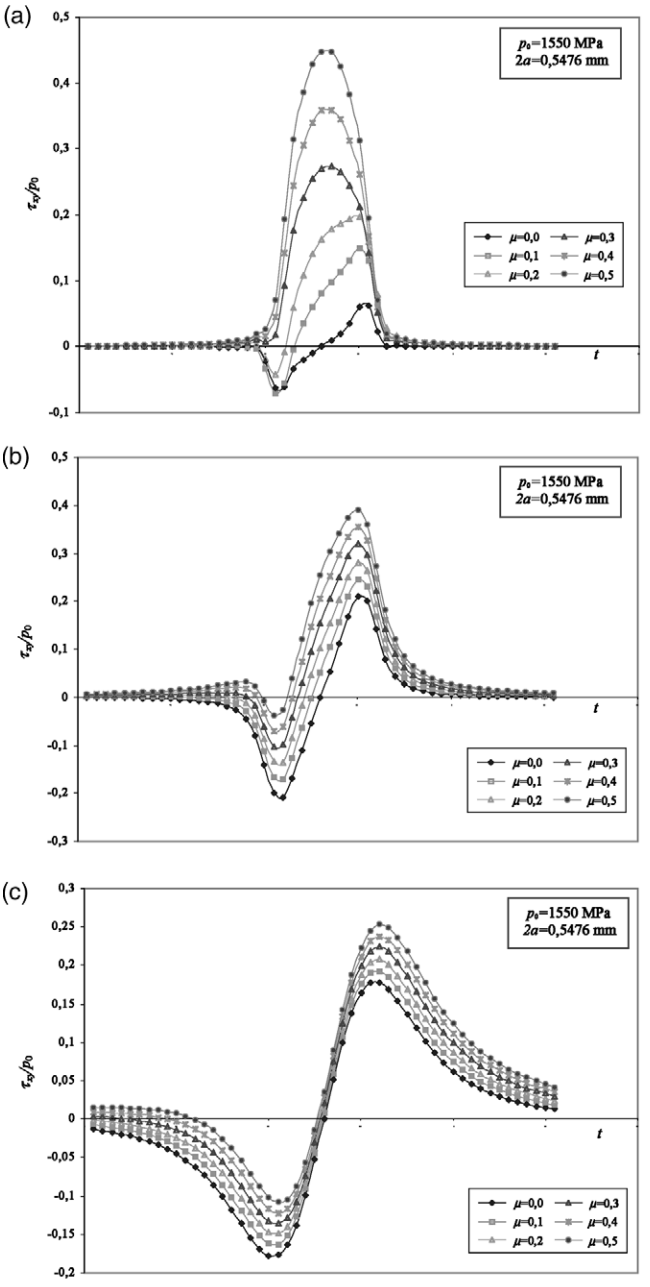

Fig. 7. (a) Loading cycles based on shear stresses τ_{xy}, on the contact surface (x_i, y_i=0 mm); (b) loading cycles based on shear stresses τ_{xy}, subsurface (x_i, y_i=−0.08523 mm);(c) loading cycles based on shear stresses τ_{xy}, subsurface (x_i, y_i=−0.3842 mm).

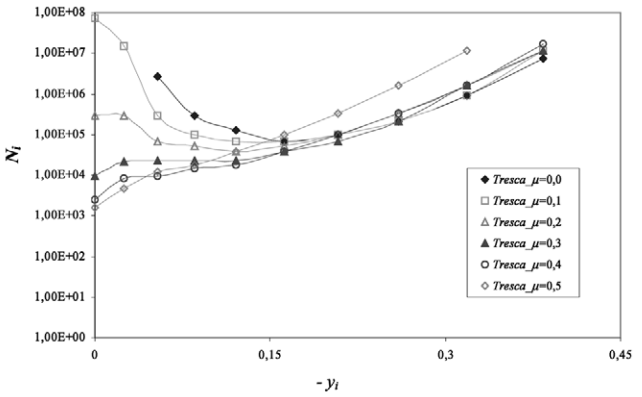

Fig. 8. Number of loading cycles, when initial crack appears at the observed material points (x_i=0, y_i) [mm]—starting-point comparative stress, $\varepsilon-N$ method of analysis.

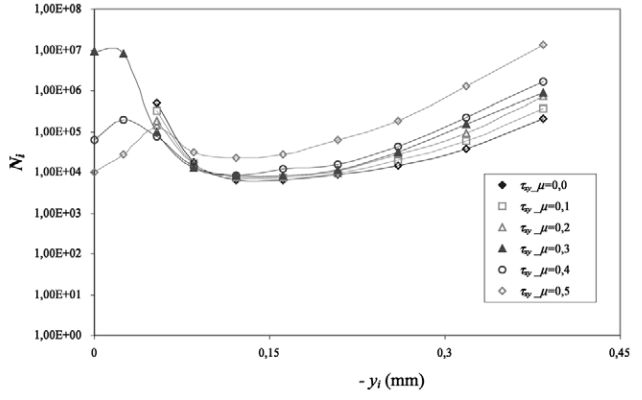

Fig. 9. Number of loading cycles, when initial crack appears at the observed material points (x_i=0, y_i) [mm]—starting-point shear stress τ_{xy}, $\varepsilon-N$ method of analysis.

at some points below the contact surface, and they are moving toward the contact surface with rising friction coefficients.

The forms of loading cycles and their characteristic values, are of significant importance for further contact fatigue analysis (Figs. 8 and 9). Using the applied relationship between specific deformation and the number of loading cycles for fatigue damage initiation, as described in Section 2 (see eq. (7)), the position of initial fatigue damage and the number of required stress cycles can be determined. For this evaluation the material fatigue parameters shown in Table 2 were used.

In this study, the fatigue analysis program MSC/Fatigue [10] has been used for computational estimation of the number of cycles for fatigue crack initiation, using described theory.

When dealing with comparative Tresca based loading cycle, the number (N_i) and place (x_i=0 mm, y_i) of the loading cycle for crack initiation should depend on the coefficient of friction μ (Fig. 8). In the case of μ=0.0 the number of loading cycles required for initial fatigue damage to appear is N_i=69813 and first occurs at point (x_i, y_i=−0.16193 mm) under the contact surface (Fig. 9).

The highest coefficient of friction causes the number of cycles N_i to reduce and the starting point of crack initiation is placed more in the direction of the contact surface. However, when dealing with shear stresses τ_{xy} based on the loading cycle (Fig. 9), the number of loading cycles required for initial fatigue damage to appear in the case of μ=0.0 is N_i=6289 and first occurs at point (x_i, y_i=−0.12126 mm) under the contact surface, respectively.

Extreme values of the coefficient of friction (μ=0.4 and μ=0.5) cause the fatigue damage to occur relatively early in the fatigue process and its place is as a rule on the contact surface.

The influence of modified strain–life methods, described in Section 2, Coffin–Manson's hypothesis ($\varepsilon-N$ method), Morrow's analysis and the Smith–Watson–Topper (SWT) method at the different coefficient of friction values is analysed in detail. The comparative Tresca based loading cycles are presented in Fig. 10(a) to (f). The number of loading cycles (for all three methods of analysis) for fatigue crack initiation is, regarding to friction coefficient, in the range of: (i) μ=0; N_i=7·10^4–2·10^6 (under contact surface $y_i\cong-0.16193$ mm) Fig. 10(a); (ii) μ=0,1; N_i=7·10^4–1.8·10^6 (under contact surface $y_i\cong-0.162$ mm) Fig. 10(b); (iii) μ=0.2; N_i=3.8·10^4–5.8·10^5 (under contact surface $y_i\cong-0.12126$ mm) Fig. 10(c); (iv) μ=0.3; N_i=9.1·10^3–5.4·10^4 (on the contact surface) Fig. 10(d); (v) μ=0.4; N_i=2.5·10^3–8.4·10^3 (on the contact surface) Fig. 10(e) and (vi) μ=0.5; N_i=1.6·10^3–4·10^3 (on the contact surface) Fig. 10(f).

The shear stress based loading cycles are presented in Fig. 11(a) to (f). In the case of all three methods ($\varepsilon-N$, SWT and Morrow) the deviation between results of loading cycles can be neglected. Minor deviation occurs at

Table 2
Fatigue material parameters for the generalised contact model

Material	Exponent of material strength b	Fatigue ductility exponent c	Fatigue ductility coefficient ε'_f	Fatigue strength coefficient σ'_f (MPa)	Material strength coefficient K' (MPa)	Material hardening exponent n'
20Mn5	−0.08	−0.51	0.28	1464	2278	0.19

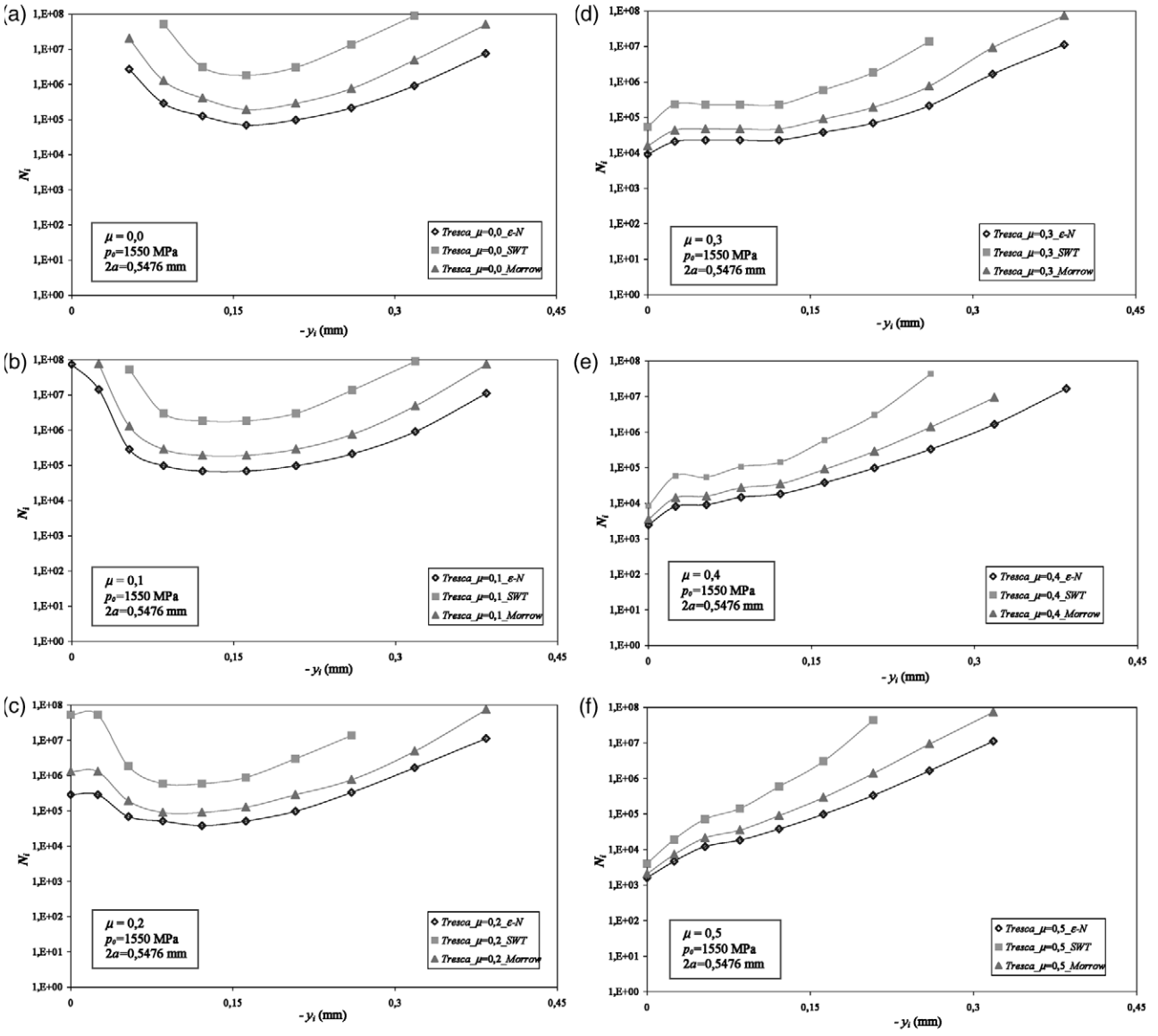

Fig. 10. (a) Number of loading cycles, when initial crack appears at the observed material points (x_i=0, y_i) [mm]—starting-point comparative Tresca stress, different methods of analysis ($\varepsilon-N$, SWT and Morrow), μ=0.0; (b) μ=0.1; (c) μ=0.2; (d) μ=0.3; (e) μ=0.4; (f) μ=0.5.

the highest friction coefficients, where the fatigue crack first initiated at the contact surface (Figs 11(d), (e) and (f)).

The motivation for dealing with different contact loading stress cycles and different criteria of fatigue initiation lies in the fact that the influence of each stress component (shear stress, comparative stress, etc.) is specific and has its origin and influence on the number of fatigue initiation loading cycles (N_i).

4. Conclusions

The numerical model of fatigue damage initiation due to contact loading of mechanical elements such as gears, bearings, wheels, etc. is presented in this paper. A simple equivalent model of a cylinder and flat surface is used for simulation of contact fatigue crack initiation under conditions of rolling and sliding contact loading. The equivalent model is subjected to the normal (normal contact pressure), see Johnson [8] and tangential (frictional forces) contact forces. The material model is assumed as homogeneous, without imperfections such as inclusions, asperities, roughness, residual stresses, etc. as often occur in mechanical elements. These drawbacks of the presented model should be improved in the analysis of practical applications (spur gears, rails etc.), where all enumerating facts actually occur in some manner. The influence of friction upon the contact loading cycle is analysed in detail. The modified strain–life method, in the framework of finite element analysis, is used for analysing the contact fatigue crack initiation. The presented

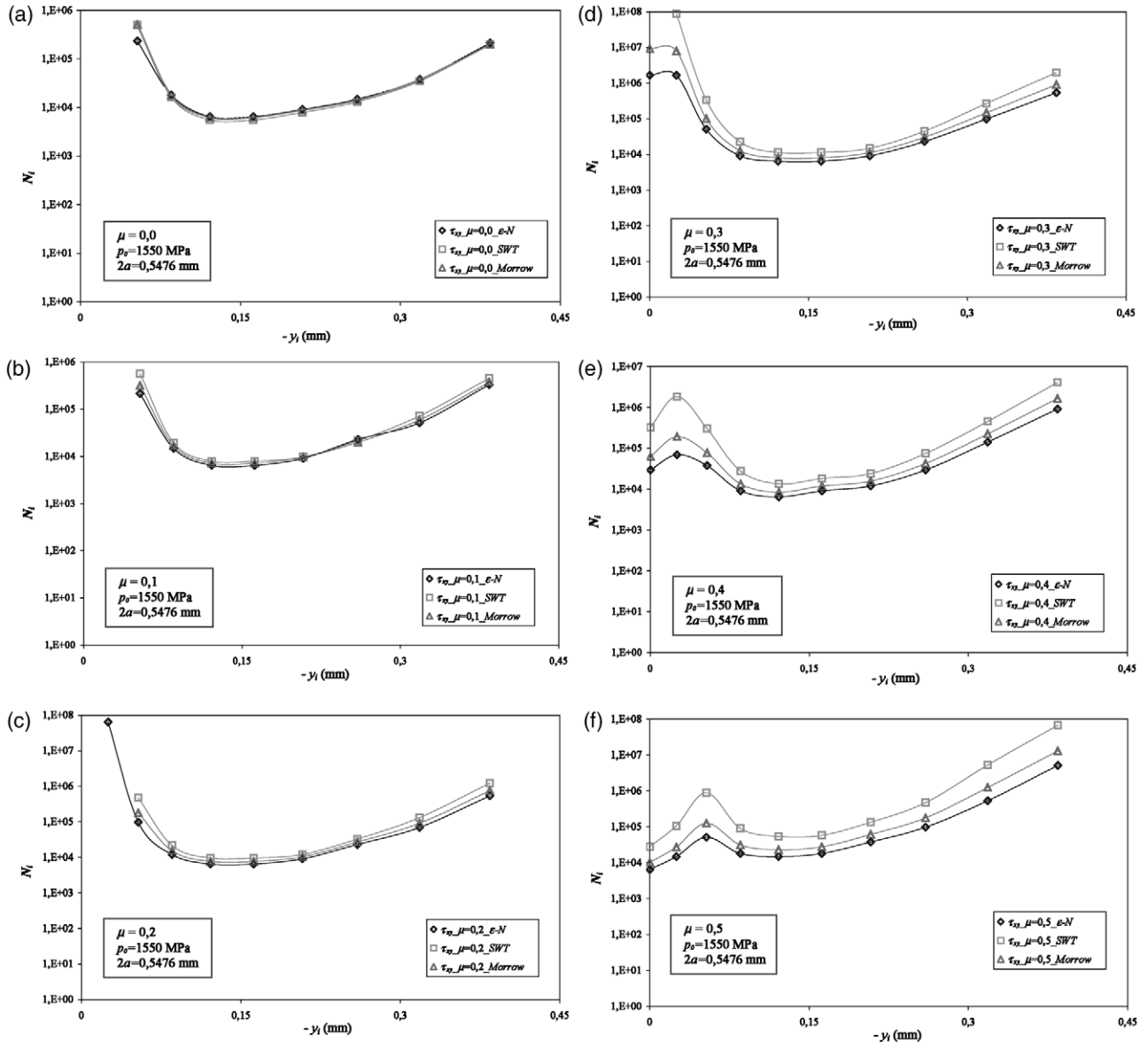

Fig. 11. (a) Number of loading cycles, when initial crack appears at the observed material points (x_i=0, y_i) [mm]—starting-point shear stress τ_{xy}, different methods of analysis ($\varepsilon-N$, SWT and Morrow), μ=0.0; (b) μ=0.1; (c) μ=0.2; (d) μ=0.3; (e) μ=0.4; (f) μ=0.5.

model provides means for determination of the number of loading cycles N_i required for fatigue damage initiation from stress loading cycles at observed material points and adequate material fatigue parameters. The computational modelling and the possibility of predicting fatigue damage initiation in contacting mechanical elements represent a major contribution to the field of contact fatigue initiation. Rolling–sliding boundary conditions on the contact surface are taken into consideration only through the influence of the friction coefficient. The deduced numerical calculation for the determination of loading cycles concerns the transition of sliding–rolling contact loading, considers different fatigue analysis approaches and specifies critical points of fatigue damage initiation, boundary conditions of geometry and loading (normal, tangential) on and under the surface. With computational experimentation it has been determined that the influence of friction can be neglected for material points at depths larger than $1.4 \cdot a$ [20]. It has been established that higher friction leads to earlier initial fatigue damage closer to the contact surface, where the limiting value of the friction coefficient for fatigue crack initiation on the contact surface is equal to 0.3. Regardless of the selected stress component, the number of loading cycles required for initial fatigue damages is in the range of N_i=(10^4–10^7) and where (on the contact surface or subsurface initiated contact fatigue) the contact fatigue damage first occurs mostly depends on the coefficient of friction, material parameters and contact geometry.

The proposed model enables the determination of the number of loading cycles N_i required for fatigue damage initiation by means of certain loading cycles and the introduction of adequate material fatigue parameters. The method of dealing with numerical modelling and the possibility of foretelling fatigue damage initiation in mechanical elements as a consequence of cyclic contact loading represents a contribution to the problems discussed.

The model can be further improved with additional theoretical and computational research, although additional experimental results are first required to verify the applicability of the model. Derivation of the analytical procedure for Hertzian time dependent contact loading should be one of the challenge tasks for further work, where some important influencing parameters, such as surface roughness, local sliding, etc. have to be taken into account. The presented computational model enables better understanding of the fatigue crack initiation process on and under the contact area since it accounts for moving rolling–sliding contact loading. The model is applicable also for the prediction of fatigue crack propagation, which can take advantage of the computed stress loading cycles in combination with the adequate fatigue crack propagation theory. The total number of loading cycles required for fatigue damage appearance can be obtained as the sum of the number of loading cycles required for crack initiation and the number of loading cycles required for crack propagation.

Nevertheless, the presented numerical model enables a better understanding of the process of fatigue crack initiation in the contact area—rolling–sliding boundary conditions on the contact surface are taken into consideration. This causes permanent damage to mechanical elements.

However, the presented model should be used for practical applicability of contact fatigue of mechanical elements, e.g. the contact fatigue of gear teeth flanks [6, 19].

References

[1] Bhattacharya B, Ellingwood B. Continuum damage mechanics analysis of fatigue crack initiation. Int J Fatigue 1998;20(9):631–9.

[2] Cheng W, Cheng HS, Mura T, Keer LM. Micromechanics modeling of crack initiation under contact fatigue. J Tribology—Trans ASME 1994;116:2–48.

[3] Ekberg A. Rolling contact fatigue of railway wheels. Ph.D. Thesis, Chalmers University of Technology, Göteborg, 2000.

[4] Ekberg A, Bjarnehed H, Lunden R. A fatigue life model for general rolling contact with application to wheel/rail damage. Fatigue Fract Eng Mater Struct 1995;18(10):1189–99.

[5] Fatemi A, Yang L. Cumulative fatigue damage and life prediction theories: a survey of the state of the art for homogeneous materials. Int J Fatigue 1998;20(1):9–34.

[6] Flašker J, Fajdiga G, Glodež S, Hellen TK. Numerical simulation of surface pitting due to contact loading. Int J Fatigue 2001;23(10):599–605.

[7] Glodež S, Flašker J, Ren Z. A new model for the numerical determination of pitting resistance of gear teeth flanks. Fatigue Fract Eng Mater Struct 1997;20:71–83.

[8] Johnson KL. Contact mechanics. Cambridge University Press; 1985.

[9] Lazzarin P, Tovo R, Meneghetti G. Fatigue crack initiation and propagation phases near notches in metals with low notch sensitivity. Int J Fatigue 1997;19(8–9):647–57.

[10] Msc/Corporation. MSC/FATIGUE quick start guide, version 8. Los Angeles: The MacNeal–Schwendler Corporation; 1999.

[11] Msc/Corporation. MSC/NASTRAN quick start guide, version 70.5. Los Angeles: The MacNeal–Schwendler Corporation; 2000.

[12] Mura T, Nakasone Y. A theory of fatigue crack initiation in solids. J Appl Mech 1990;57:1–6.

[13] Bishop NWM, Sherratt F. NAFEMS. Finite element based fatigue calculations. Farnham: The International Association for the Engineering Analysis Community; 2000.

[14] Potrč I, Franko D. An elasto–plastic boundary element simulation of two-dimensional rolling contact. Z angew Math. Mech 1993;73(4–5):366–9.

[15] Ren Z, Flašker J. Nonlinear contact analysis of harmonic gear drive. In: Proceedings of the 4th International Conference on Nonlinear Engineering Computations (NEC91). Swansea: Pineridge Press; 1991. p. 481–90.

[16] Ringsberg JW, Loo-Morrey M, Josefson BL, Kapoor A, Beynon JH. Prediction of fatigue crack initiation for rolling contact fatigue. Int J Fatigue 2000;22:205–15.

[17] Shang DG, Yao WX, Wang DJ. A new approach to the determination of fatigue crack initiation size. Int J Fatigue 1998;20:683–7.

[18] Suresh S. Fatigue of materials, 2nd ed. Cambridge: Cambridge University Press; 1998.

[19] Šraml M. Modeling of contact fatigue of mechanical elements. Ph.D. Thesis, Abstract in English, Maribor, Slovenia, 2001.

[20] Šraml M, Flašker J, Potrč I, Ren Z. Generalised computational analysis of contact fatigue initiation of mechanical elements. In: Blom AF, editor. Fatigue 2002, Proceedings of the eighth international fatigue congress, Stockholm, Sweden, vol. 3. EMAS; 2002. p. 2167–74.

[21] Zahavi E, Torbilo V. Fatigue design-life expectancy of machine parts. Florida: A Solomon Press book by CRC Press; 1996.